Fault ride through study of doubly fed induction generator wind turbine in real-time simulation environment

A.S. Mäkinen, P. Lauttamus, O. Raipala, S. Repo, H.Tuusa
TAMPERE UNIVERSITY OF TECHNOLOGY
Korkeakoulunkatu 3, FI-33101
Tampere, Finland
Tel.: +358 – 401981522
E-Mail: anssi.makinen@tut.fi
URL: www.tut.fi/set

Keywords

«Fault ride through», «Wind energy», «Real time simulation», «Converter control», «AC machine»

Abstract

In this paper, the fault ride through (FRT) of the doubly fed induction generator (DFIG) wind turbine is studied. The study is done by using a simulation environment in which the network is simulated using Real-Time Digital Simulator (RTDS) and the wind turbine is simulated using dSPACE in real time. The effect of transient flux on the operation of the wind turbine during a network voltage dip is analyzed. The simulation results show that the network voltage support can be maximized if the transient flux is compensated. In addition, it is proposed that different crowbar resistances should be used during the voltage drop and the voltage recovery in order to avoid network short-term voltage stability problems.

Introduction

The latest grid codes insist that wind turbines should have capability to stay in operation in case of a network voltage dip. Furthermore, the wind turbines should be able to inject reactive power to the grid during the voltage dip in order to support the network voltage. In this study, the fault ride through (FRT) and the reactive power generation capabilities of the doubly fed induction generator (DFIG) wind turbine concept, Fig. 1, is investigated. In the stationary state, the amplitude of the rotating magnetic flux of the DFIG is proportional to the stator voltage. A voltage dip in the stator terminals decreases the amplitude of the rotating flux instantaneously and generates a non-rotating transient flux component which gets its maximum value at the beginning of the voltage step. The induced voltage to the DFIG rotor is proportional to the angular slip frequency i.e., the difference between the synchronous angular frequency of the flux and the rotor electrical angular speed. Because the angular frequency of the transient flux component is zero the transient flux creates very high rotor voltages. A deep network voltage dip induces higher voltages to the rotor circuit than the rotor side converter (RSC) can generate from the DC-link voltage. [1] Thus, the RSC cannot control the rotor currents anymore and the currents can't be limited. Typically, the RSC is disconnected from the rotor circuit and the crowbar, i.e. a set of resistors, is used to decrease the rotor currents and protect the sensitive converter.

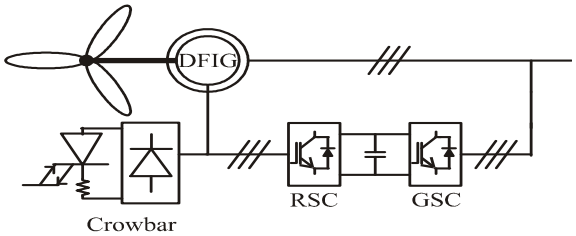

Fig. 1. The DFIG wind turbine concept.

Crowbar protection

Normally, the RSC supplies the magnetizing current of the generator, but after the connection of the crowbar in the rotor circuit, the reactive power for the magnetization is taken from the grid. The crowbar can be switched off after the rotor voltages have decreased so much that the rotor currents can be controlled again during the voltage dip by using the RSC. High rotor currents, torque stresses and grid currents appear as a result of the voltage dip if very low value of the crowbar resistance is used. However, if a too high value of crowbar resistance is used, very high voltages appear in the rotor circuit which may damage the isolation of the rotor windings. In addition, the rotor currents may start to flow to the DC-link of the frequency converter if the rotor voltages become higher than the DC-link voltage. [2]

The behavior of the DFIG during the network voltage recovery has received surprisingly little amount of attention in the literature. When the network voltage recovers, the rotor currents will increase again and the RSC should be protected from the overcurrents. One possible solution is the crowbar re-activation. [3][4][5] Then, the active and reactive powers of the generator are determined by the slip and terminal voltage.[6] However, the rotor resistance has a remarkable influence on the steepness of the slip-torque curve of the generator.[4] Thus, if too low crowbar resistance is used, the consumed reactive power of the DFIG during the voltage recovery is very high. This may cause short-term voltage stability problems if there is no reactive power source such as STATCOM installed near the turbine. The problems are more severe in weak networks or in the case of wind farms.[7] Thus, it is highlighted in [8] that the second crowbar connection should be avoided in all possible cases. In order to avoid the crowbar activation during a voltage recovery the braking chopper installed in the DC-link of the frequency converter can be used to protect the DFIG.[9] However, the rotor currents flow through the antiparallel diodes to the DC-link which need to be taken into account when dimensioning the power components. Also, the DC-link needs to be protected from the overvoltages.

The selection of correct crowbar resistance has been studied in several papers. The correct choice of the crowbar resistance depends on the generator parameters. Thus, different generators may need differently sized crowbar resistances. However, the range of the proposed resistance values in the literature is huge. In [2], the proposed crowbar resistance value is 0.05p.u. The study doesn't take into account the voltage recovery and if the crowbar would be activated during the voltage recovery the short-term voltage instability problems may appear. In [4], the crowbar was selected to take also the voltage recovery into account and the size was selected to be 0.5p.u. However, the simulation results in [4] show that the terminal voltages cannot be restored after the voltage recovery. Crowbar resistances sized in the middle of values 0.05-0.5p.u can be found from the references [10][11].

Transient flux compensation control

Xiang *et. al*. [12] proposes a method where the RSC generates rotor currents that oppose the transient flux during the voltage dip. The purpose is to cancel the transient flux in order to avoid the rotor voltages to exceed the DC-link voltage. Lopez *et. al*. [3] uses also currents that oppose the transient flux. However, they also point out that the amount of the demagnetizing current needed to cancel the transient flux is very high. Thus, the RSC should be over dimensioned to have large current capacity. This fact, however, is against of the advantage of the DFIG which is small converters.

In this paper, the fault ride through (FRT) process relies on the combination of the crowbar protection and the transient flux compensation. The aim is to investigate what is the influence of the transient flux on the operation of the DFIG during a symmetrical voltage dip. It is shown, that the compensation of the transient flux is beneficial from the power quality and the network voltage support viewpoints. The influence of the crowbar resistance selection is also analyzed. It is presented that major short-term voltage instability problems in the network during the voltage recovery may occur if too low crowbar resistance is used. A solution, where the second crowbar activation can be done without the voltage instability problems, is presented. The key of the solution is the use of two different crowbar resistances depending on whether the voltage drops or recovers.

Modeling and control of DFIG wind turbine

The space-vector based equivalent circuit of the modelled DFIG is presented in Fig. 2a. The stator of the generator is directly connected to the grid while the rotor circuit is connected to the grid via RSC and grid side converter (GSC). Variables with superscript ‘ are reduced to the stator. The transformer describes the rotor to stator turns ratio of the generator. Both the RSC and the GSC are assumed to operate in the linear modulation area. The converters are assumed to execute their voltage reference ideally i.e., the switching performance is not modelled in order to save the calculation resources. The saturation of the 0.69/21kV transformer is not taken into account. The parameters of the generator, the DC-link capacitor, the LCL-filter and the transformer are depicted in Table I. The network model is presented in Fig. 2b. The network model is a greatly simplified model of a real Finnish distribution network. High voltage network is modelled as a voltage source behind the RL-impedance.

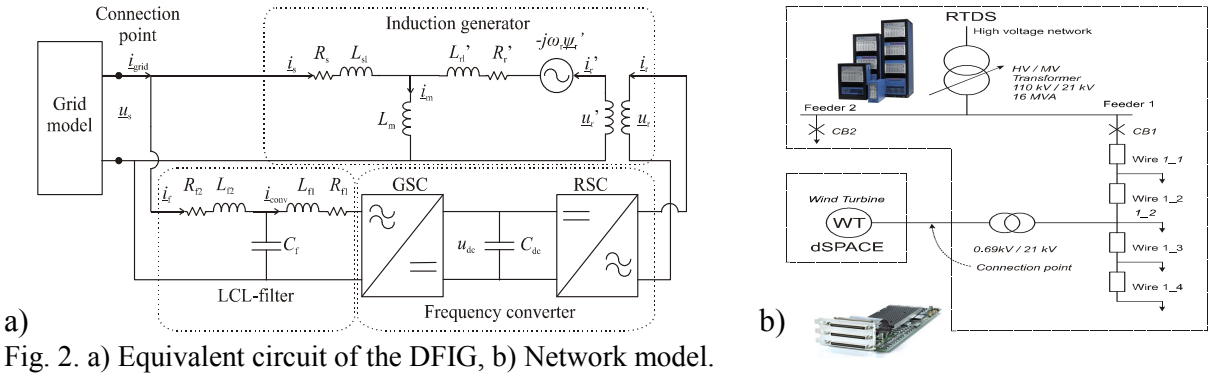

a) b)

Fig. 2. a) Equivalent circuit of the DFIG, b) Network model.

Table I: Parameters of DFIG and transformer

Generator	P_n=1700kW	$u_{s\ ll}$=690V	R_s=2.7mΩ	R_r=2.6mΩ	L_{sl}=89μH	L_{rl}=92μH
	L_m=3.8mH	p=2	(pole pairs)	N_r/N_s=2.73	(turns ratio)	
LCL-filter	L_{f1}=190μH	L_{f2}=125μH	R_{f1}=15mΩ	R_{f2}=5mΩ	C_f=70μF	
Converter	u_{dc}^{ref}=1100V	C_{dc}=22mF				
Transformer	u_1=21kV	u_2=0.69kV	S_n=1.75MVA	X_k=6%	R_k=1%	
Transformer	u_1=110kV	u_2=21kV	S_n=16MVA	X_k=10.3%	R_k=0.6%	
High voltage network		u=110.4kV	R=19.8Ω	X=44Ω		

Control system

The control system of the wind turbine includes the RCS control, GSC control and pitch control. The pitch control system is used to curtail the wind power production during high wind speeds in order to reduce the load of the mechanical and the electrical parts of the turbine system. The pitch control system used in this study is presented in [13].

Grid side converter control

The GSC control is done in the reference frame oriented to the positive sequence component of the connection point voltage vector $\underline{u}_s$. The voltage vector component is extracted using a dual second order generalized integrator–frequency-locked loop (DSOGI FLL), Fig 3. [14]

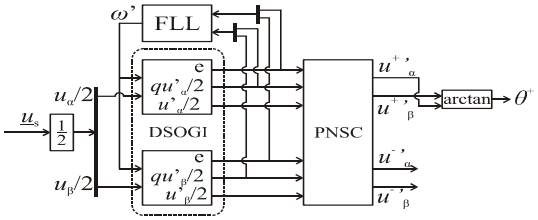

Fig. 3. Schematic diagram of the DSOGI-FLL.

The DSOGI is a bandpass filter. Output signals, v_α’, v_β’, qv_α’ and qv_β’, are used to calculate the positive and the negative sequence (PNS) components of the grid voltage. The PNS components can be estimated accurately as long as the filter resonance frequency ω’ corresponds to the grid frequency.

Because the grid frequency is not constant the FLL is used to modify the filter resonance frequency to the grid frequency. Thus, the DSOGI-FLL is a filter adapted to the grid frequency and its outputs are used to detect the PNS components of the grid voltage vector.

The control system of the GSC is illustrated in Fig. 4. The fast inner loop controls the converter current components $i_{conv,x}$ and $i_{conv,y}$. The aim of the DC-link voltage controller is to keep the constant DC-link voltage u_{dc}, thereby ensuring the active power balance between the RSC and the GSC. The output of the DC-link voltage controller is the reference of the converter active current component $i_{conv,x}$*. In the normal operation, the reference of the converter reactive current component $i_{conv,y}$* is set to zero. However, the reference may be modified if reactive power generation during a voltage dip is wanted. The output of the control system is the reference for the converter voltage vector $\underline{u}_{conv}$*.

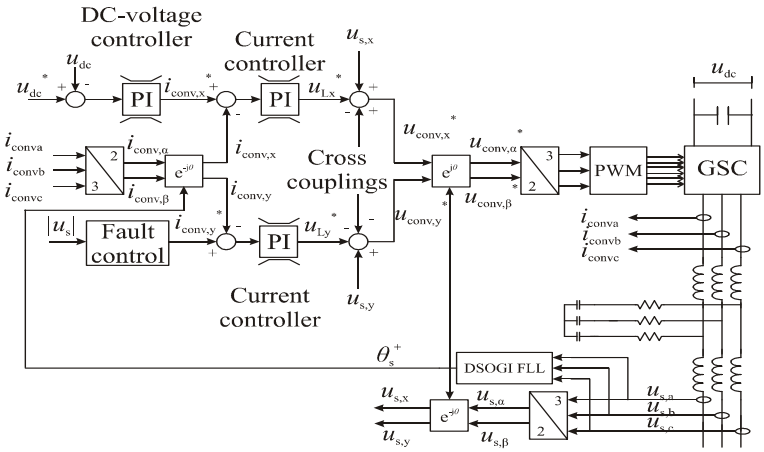

Fig. 4. Control system of the GSC. [15]

Rotor side converter control

The control system of the RSC is illustrated in Fig. 5. The control is based on vector control in a reference frame that is oriented to the estimated positive sequence component of the stator flux linkage. The stator flux linkage is calculated in calculation block from the measured stator voltages and currents. Then, the PNS components of the stator flux linkage are estimated using the DSOGI-FLL. The RSC is controlled so that the DFIG extracts the maximum power from the wind by producing such a torque that optimizes the ratio between the blade tip speed and wind speed. The output of the speed controller is the torque reference t_e*. The torque controller gives the reference value for the rotor current y-component i_{ry}*. The reactive power controller controls of the reactive power exchange with the grid and it gives the reference for the rotor current x-component i_{rx}*. The cross coupling compensation terms are added to the outputs of the current controller and the references for the rotor converter voltage vector components u_{rd}* and u_{rd}* are achieved.

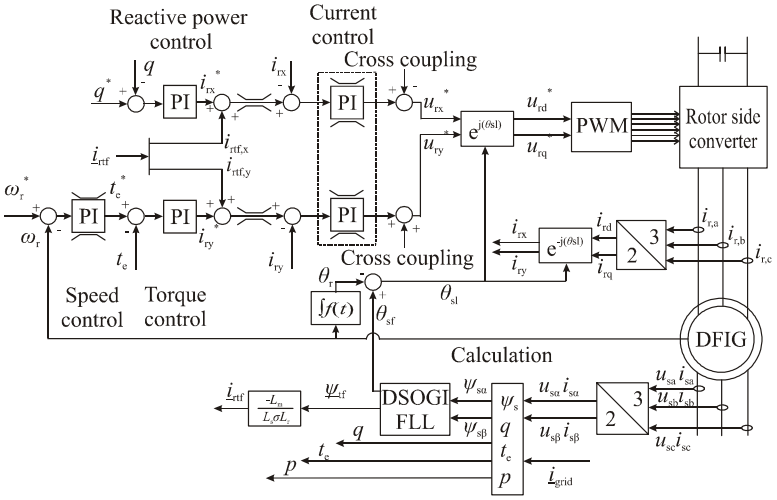

Fig. 5. Control system of the RSC. [15]

Transient flux compensation control

The DSOGI-FLL is used to calculate the positive sequence component from the stator flux linkage. In the case of the symmetrical voltage dip, the transient flux linkage $\underline{\psi}_{tf}$ is the difference between the total stator flux linkage $\underline{\psi}_s$ and the positive sequence component of the flux linkage $\underline{\psi}_{s+}$.

$$\underline{\psi}_{tf} = \underline{\psi}_s - \underline{\psi}_{s+} \tag{1}$$

The stator and the rotor flux linkage can be expressed using Equations:

$$\underline{\psi}_s = L_s \underline{i}_s + L_m \underline{i}_r \tag{2}$$

$$\underline{\psi}_r = L_r \underline{i}_r + L_m \underline{i}_s \tag{3}$$

where $\underline{\psi}_r$ is the rotor flux linkage, L_s and L_r are the stator and the rotor self-inductances, respectively, and L_m is the magnetizing inductance. The stator and rotor currents are $\underline{i}_s$ and $\underline{i}_r$, respectively. The rotor flux linkage can be expressed using (2) and (3): [12]

$$\underline{\psi}_r = \underline{\psi}_{r+} + \underline{\psi}_{rtf} = \frac{L_m}{L_s}\underline{\psi}_s + L_r \underline{i}_r - \frac{L_m^2}{L_s}\underline{i}_r = \frac{L_m}{L_s}\underline{\psi}_s + \sigma L_r \underline{i}_r = \frac{L_m}{L_s}\left(\underline{\psi}_{s+} + \underline{\psi}_{tf}\right) + \sigma L_r \left(\underline{i}_{r+} + \underline{i}_{rtf}\right) \tag{4}$$

where σL_r is defined as the rotor transient inductance [$\sigma L_r = L_r - (L_m^2/L_s)$]. The current $\underline{i}_{rtf}$, Fig. 5, that oppose the transient flux $\underline{\psi}_{tf}$ can be calculated using (4) and setting $\underline{\psi}_{rtf}=0$.

$$\underline{i}_{rtf} = -\frac{L_m}{L_s \sigma L_r}\underline{\psi}_{tf} \tag{5}$$

The idea behind the FRT concept is to control the RSC currents to minimize the effect of the transient flux on the rotor. Thus, the transient flux compensation current is prioritized. After the transient flux is removed the current capacity of RSC can be utilized for reactive power generation.

Crowbar protection during voltage recovery

Typical active crowbar protection structure is illustrated in Fig. 1. [3] The crowbar consists of a diode bridge and an additional resistance which is connected to the rotor circuit if the switch is closed. The switch is based on IGBTs (insulated gate bipolar transistor) or GTOs (gate turn off thyristor). When the crowbar is connected to the rotor circuit the DFIG behaves like an ordinary induction generator with high slip and increased rotor resistance. The active and the reactive power of the induction generator are determined by the slip speed and the terminal voltage as can be seen from the Fig. 6a. The rotor resistance has great impact on the torque and the reactive power of the generator as depicted in the Fig. 6b. It can be seen that the lower the rotor resistance is the steeper the slip-torque curve is. Low crowbar resistance is proposed in many papers (from 0.05 to 0.5p.u.) because that way the high slip ring voltages after a voltage dip can be avoided. However, when the terminal voltages return, the generator consumes huge amount of reactive power when low crowbar resistance is used and the generator operates with high slip speed. Thus, the stator currents become very high which causes significant voltage drop on the network impedances. Naturally, the voltage drop is proportional to the network impedance and thus the voltage problems are more severe in the weak networks.

The significant voltage drop due to high stator currents decreases the DFIG terminal voltage even while the network voltage has been recovered. Hence, the pull-out torque of the generator decreases which may lead to the acceleration of the turbine. If the speed of the turbine increases above the pull-out slip the turbine needs to be tripped due to the excessive reactive power consumption of the generator as can be seen from Fig. 6a. That would fail the FRT process. However, the pitch control can be used to counteract against the acceleration.

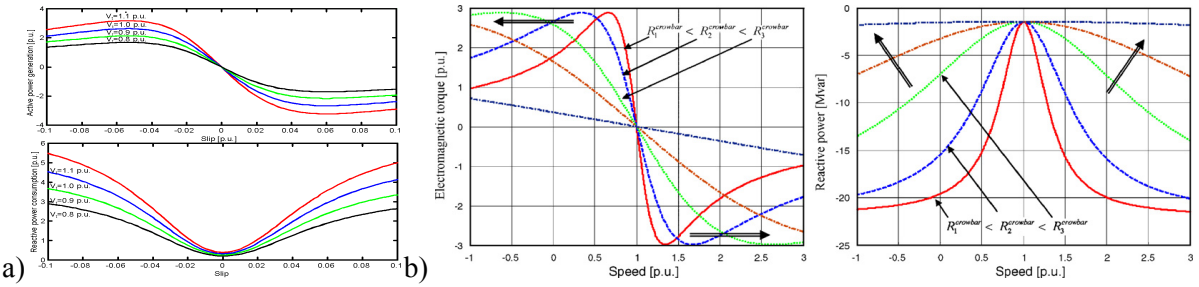

a) b)

Fig. 6. a) The active and the reactive power of the induction generator with respect to the slip and the terminal voltage [6], b) The influence of the crowbar resistance on the slip-torque curves and the reactive power [4].

Based on the discussion above, it seems evident that the use of too low crowbar resistance may cause voltage short-term instability during the voltage recovery. However, it is not allowed to increase the crowbar resistance without restrictions because it would cause unacceptable high slip ring voltages after the voltage dip. The proposed solution to the problem is the use of two different resistances depending on whether the voltage drops or recovers. The modification to the crowbar structure is illustrated in Fig. 7. During a normal operation the switch S2 is closed. When the voltage dip occurs the crowbar is activated by closing the switch S1. When the voltages on the rotor side have decreased the switch S1 can be opened again and the RSC can be used to control the operation of the DFIG even there is a low voltage in the network. After that, the switch S2 is opened. When the network voltages recover and the crowbar is activated by closing the switch S1 the crowbar resistance is the sum of the resistances R1 and R2. The switch S1 is typically based on IGBTs or GTOs when the active crowbar protection is desired. The switch S2 can be based on GTOs or IGBTs as well. This arrangement would provide stepless control of the crowbar resistance. However, if a more cost effective solution is wanted, a simple contactor based switch may be used because no actual need for stepless control of the resistance is needed.

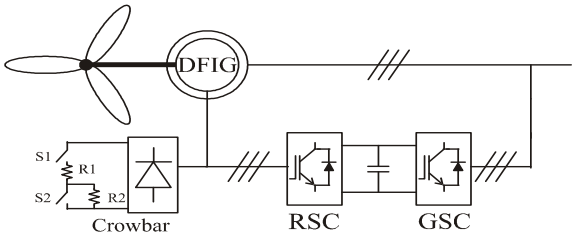

Fig. 7. Proposed crowbar structure.

Real-time simulation environment

The combination of the power system simulator (RTDS) and a control system simulator (dSPACE) provides excellent environment for wind turbine and network interaction studies. The simulation environment used makes it possible to develop control strategies for wind turbines to qualify more demanding grid codes in the future with minimized simulation time. It is also possible to include real physical devices in the simulations.

Figure 8 shows the block diagram of the RTDS/dSPACE implementation. The DFIG is modelled in Simulink and based on the model dSPACE runs the simulation in real time. The ControlDesk software is used to control and observe the simulation. The power system model is created in RSCAD Draft mode. RSCAD Runtime mode is used to control the real time simulation that is performed by RTDS. Data transmission between the real time simulators is done through analog signals. In other words, first digital signals of the simulator are converted to analog signals which are converted back to digital signals when fed to the other simulator. The signal *int* is a hardware interrupt signal required to synchronize the calculations of the two simulators. The dSPACE receives the connection point voltages $u_{s(a,b,c)}$ and the interruption signal from the RTDS and gives the connection point current $i_{grid(\alpha,\beta)}$ back. From the RTDS viewpoint, the wind turbine is modelled as a current source. The hardware arrangement of the environment is shown in Fig. 9.

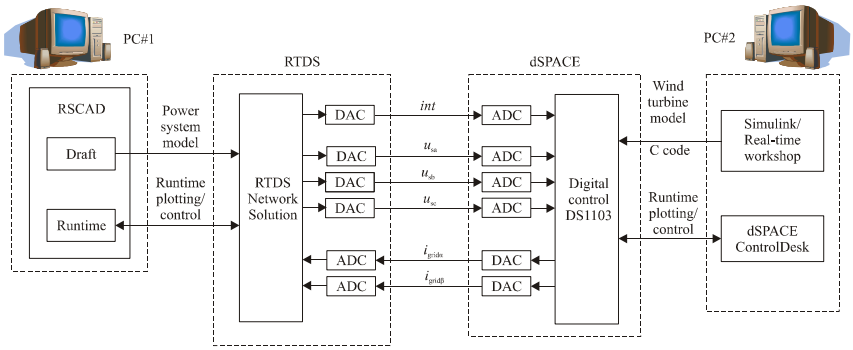

Fig. 8. The block diagram of the RTDS/dSPACE implementation.

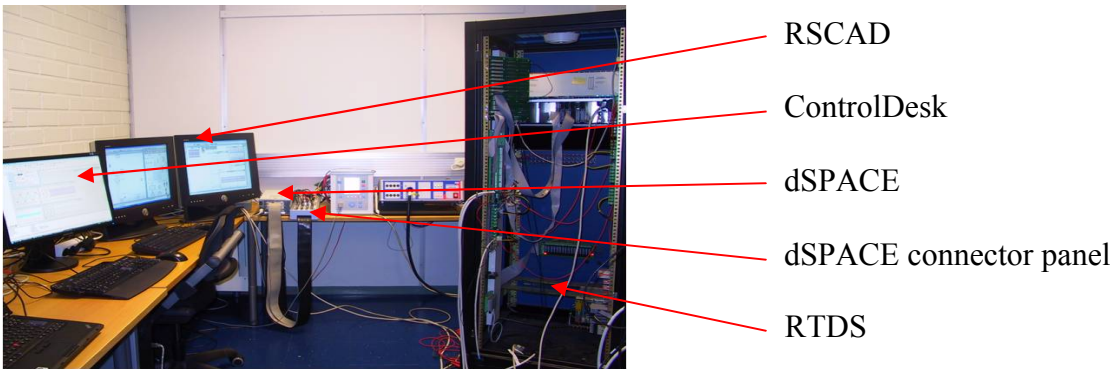

Fig. 9. Hardware arrangement of the real-time simulation system.

The interface between the simulators is chosen to allow simple and flexible interconnection of devices such as wind turbine, STATCOM or active filter to the network. Every device model is run by its own dSPACE and many dSPACEs can be connected to the RTDS network simultaneously. Thus, complex models can be built because the calculation power is shared between several simulators. For example, it would be reasonable to model all electrical parts in the RTDS and the control system in the dSPACE. However, that would reduce the expandability of the RTDS model in future studies.

Simulation results

The three-phase voltage dip with residual voltage of 20% of the nominal value occurs on the high voltage network, Fig. 2b, and lasts 300ms. Two situations are simulated. The FRT strategy used in the first situation relies only on active crowbar protection. The protection uses the proposed modificated crowbar structure presented in Fig. 7. After the voltage dip, the crowbar resistance is 0.4p.u. After the voltage recovery the total crowbar resistance is 0.8p.u. The crowbar is activated if the measured rotor currents exceed the current feeding capacity of RSC which in this case is 900 A rms (1270A peak value). In both situations, the GSC starts to feed reactive current to the grid after voltage dip is sensed. The active current component is prioritized in order to keep the DC-link voltage in the desired value. Thus, the difference between the GSC current capacity, i.e. 600 A rms, and the measured active current is set as the reference for the reactive current component of the GSC.

The connection point voltages are illustrated in Fig. 10a. As a result of the voltage dip, the transient flux appears on the airgap of the generator. The transient flux presented in rotating coordinates oriented to the positive sequence component of the stator flux is shown in Fig. 10b. The transient flux causes high frequency oscillations to the rotor voltages as can be seen from the Fig. 10c. The rotor currents increase as a result of the voltage dip and the crowbar protection is activated as shown in Fig. 11a. After the currents have decreased enough so that the RSC can handle them, the crowbar is deactivated and the RSC is connected back in to operation. However, the transient flux causes distortion to the rotor currents. The reactive current is ramped up after crowbar removal and the active current component is set to zero. The RSC active (y-component) and the RSC reactive (x-component) currents on the reference frame oriented to the positive sequence component of the stator flux and their control references are expressed in Figs. 11b and 11c, respectively. The measured current does not

reach the reference because the presence of the transient flux causes oscillations to the currents around their references. Due to the oscillations, the reference for reactive current component is set to be lower (i.e. 1070 A) than the current capacity of the RSC (i.e. 1270A). If the reactive current reference is set to 1270 A, the measured current would be temporarily much higher than the RSC current limit due to the oscillations. That would undesirably activate the crowbar protection repetitively. The electrical torque shows oscillations as illustrated in Fig. 12a which cause additional stresses to the mechanical system. The negative value of the oscillating reactive power in Fig. 12b means that the reactive power is generated. It should be noticed from the Fig. 12c that the grid currents are not symmetrical.

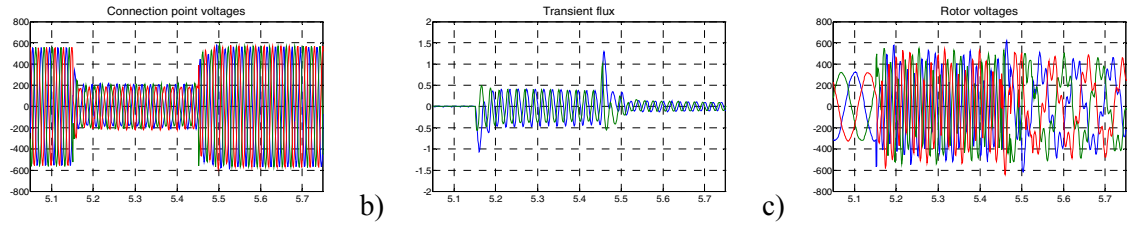

a) b) c)

Fig. 10. Without compensation: a) connection point voltages, b) transient flux, c) rotor voltages.

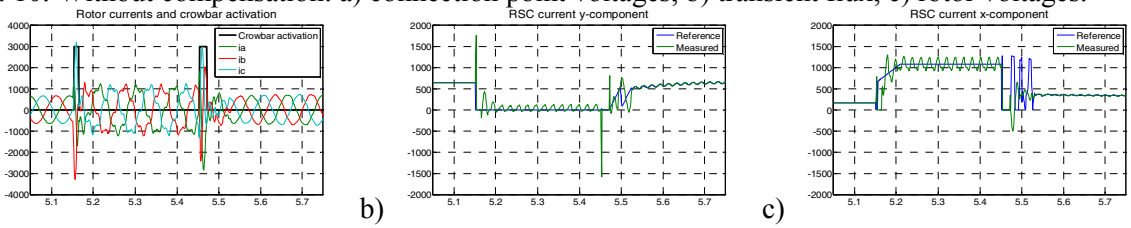

a) b) c)

Fig. 11. Without compensation: a) rotor currents and crowbar activation, b) RSC current y-component and its reference, c) RSC current x-component and its reference.

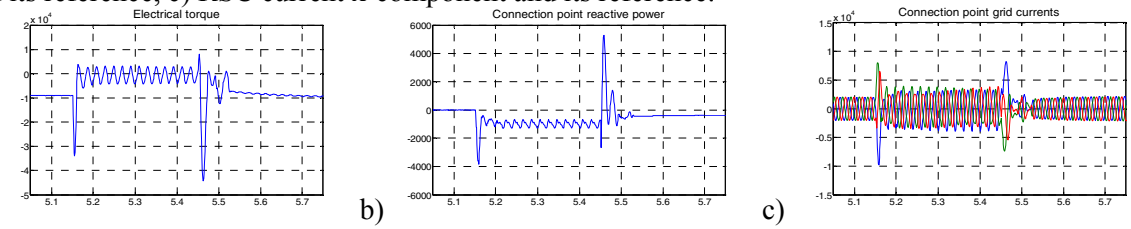

a) b) c)

Fig. 12. Without compensation: a) electrical torque, b) reactive power, c) grid currents.

Next, the same case is simulated using the active crowbar protection and the transient flux compensation control. When the crowbar is deactivated after the voltage dip, the calculated current components $i_{\mathrm{rtf,x}}$ and $i_{\mathrm{rtf,y}}$ in (5) is added to the references of the RSC currents. In addition, the active current component of the RSC is set to zero and the reactive current component of the RSC is ramped up like in previous case. The connection point voltages are depicted in Fig. 13a. Because the transient flux, Fig. 13b, is removed, the voltages in the rotor circuit do not contain high frequency oscillations as can be seen from Fig. 13c. Furthermore, the rotor currents are not distorted anymore, Fig. 14a. Compared to operation without transient flux compensation, there are no oscillations in the RSC active and reactive current components which are presented in Figs. 14b and 14c. Hence, the reference for the reactive current-component can be set to 1270 A without a fear of the crowbar reactivation. Thus, the generation of the reactive power, Fig 15b, is maximized. In addition, there are no oscillations on the generator torque expressed in Fig. 15a. Due to the absence of the transient flux the grid currents shown in Fig. 15c are symmetrical which implies improvement on the power quality.

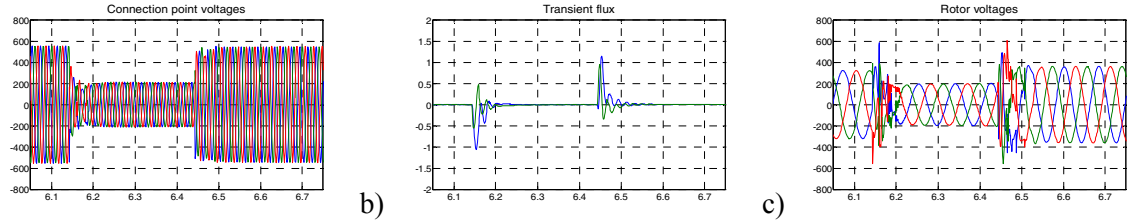

a) b) c)

Fig. 13. With compensation: a) connection point voltages, b) transient flux, c) rotor voltages.

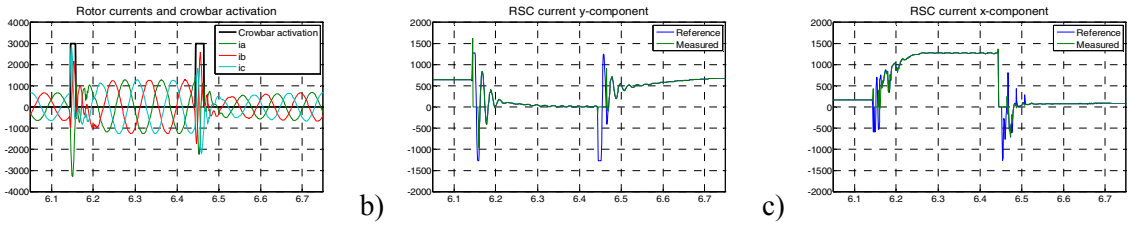

a) b) c)

Fig. 14. With compensation: a) rotor currents and crowbar activation, b) RSC current y-component and its reference, c) RSC current x-component and its reference.

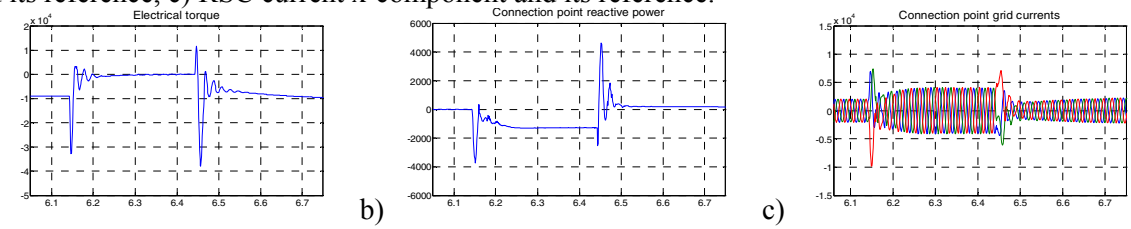

a) b) c)

Fig. 15. With compensation: a) electrical torque, b) reactive power, c) grid currents.

Impact of crowbar resistance

In both of the simulation cases presented above, the crowbar protection structure presented in Fig. 7 was used. It can be clearly seen that the voltage recovery did not pose significant problems on the network voltage stability and the reconnection time of the crowbar was short. In the next cases, the traditional crowbar structure depicted in Fig. 1 is used with transient flux compensation.

The connection point voltages when the crowbar resistance is selected to be 0.5p.u are depicted in Fig. 16a. After the network voltage recovery the crowbar is connected to protect the RSC. Due to the low crowbar resistance the rotor currents are high which prolong the crowbar connection time because the crowbar is removed only after the rotor currents are decreased enough as shown in Fig. 16c. During the crowbar activation, the reactive power is taken from the grid to magnetize the generator. The reactive power demand is high because the torque-slip curve of the generator is steep in case of low rotor resistance, Fig. 6b. Thus, high post fault grid currents, Fig. 16b, appear which cause voltage drop over the network impedance. Hence, the connection point voltage after the voltage recovery remains under the pre-fault value. When very low crowbar resistance (0.05p.u.) is used, very high rotor currents appear after the voltage recovery, Fig. 17c. Also, the crowbar reconnection takes longer time. Due to the steeper torque-slip curve and higher reactive power consumption the grid currents have increased as shown in Fig. 17b. This causes major voltage problems as depicted in Fig. 17a. This kind of behavior of the wind turbines cannot be tolerated in any case because this local short-term voltage instability may escalate to a voltage collapse in a significant part of the power system. Unlike in real power system, the reactive power reserves are unlimited and infinite quick in the simulations. Thus, in reality, it may take even longer time for the connection point voltages to recover.

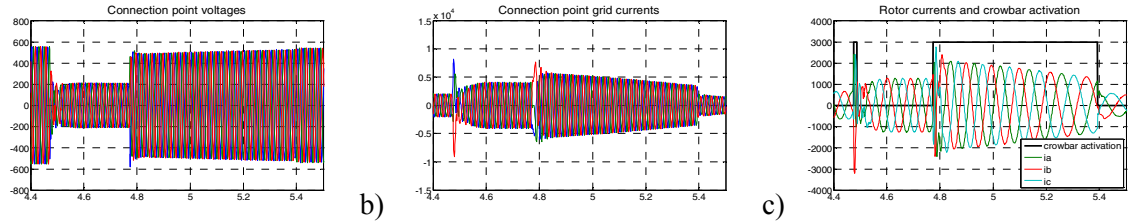

a) b) c)

Fig. 16. R_{crow}=0.5p.u.: a) connection point voltages, b) grid currents, c) rotor currents.

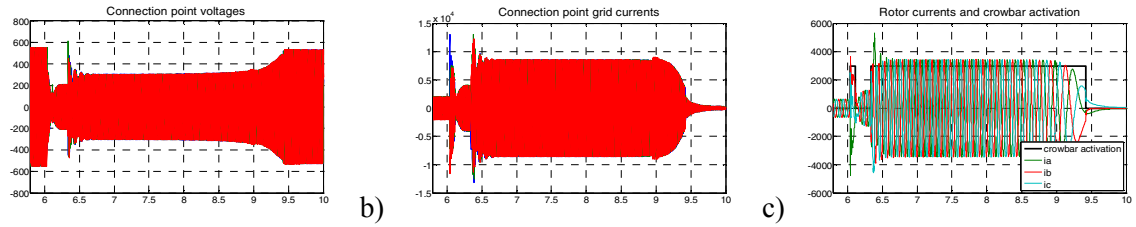

a) b) c)

Fig. 17. R_{crow}=0.05p.u.: a) connection point voltages, b) grid currents, c) rotor currents.

Conclusion

The FRT and the reactive power generation of the DFIG wind turbine are studied in this paper. The simulation studies are carried out using a real-time simulation environment including dSPACE and RTDS. If only the active crowbar protection is used during a voltage dip, the presence of the transient flux causes oscillations to the RSC active and reactive current components around the current references. Due to the oscillations, the reference value of the reactive current component is set to be lower than the current capacity of the RSC in order to avoid undesirable repetitive crowbar activation. However, if the transient flux is compensated, it is possible to utilize the whole current capacity of the RSC for reactive current injection to the grid. This aspect is important because the latest grid codes require reactive power generation to the grid during a voltage dip in order to support the network voltage. Besides, if the wind turbines generate reactive power during the voltage dips, the additional reactive power sources may not need to be installed in the network which is economically important.

The impact of the crowbar resistance on the operation of the DFIG is also studied. It is shown, that if too low crowbar resistance is used, the reactive power consumption of the DFIG during a voltage recovery can be huge. That may cause short-term network voltage stability problems especially in weak networks or in case of wind farms. It is shown, that the crowbar can be activated during the network voltage recovery without the voltage instability problems if two different crowbar resistances are used depending on whether the voltage drops or recovers.

References

[1] Lopez J, Sanchis P, Roboam X, Marroyo L.: Dynamic behavior of the doubly fed induction generator during three-phase voltage dips, IEEE Transactions on Energy Conversion, Vol. 22 no 3, 2007, pp. 709-717

[2] Morren J, De Haan S.W.H.: Short-circuit current of wind turbines with doubly fed induction generator, IEEE Transactions on Energy Conversion, Vol 22, no 1, 2007, pp.174-180

[3] Lopez J, Gubia E, Olea E, Ruiz J and Marroyo L.: Ride through of wind turbines with doubly fed induction generator under symmetrical voltage dips, IEEE Transactions on Industrial Electronics, Vol. 56, no 10, 2009, pp. 4246-4254

[4] Hansen A. D., Michalke G.: Fault ride-through capability of DFIG wind turbines, Renewable Energy Vol 32, issue 9, 2007, pp. 1594-1610

[5] Sun T, Chen Z, Blaabjerg F.: Voltage recovery of grid-connected wind turbines with DFIG after a short-circuit fault, 35th Annual IEEE Power Electronic Specialists Conference 2004, pp. 1991-1997

[6] Kling W. L, Slootweg J.G.: Wind turbines as power plants, Workshop on Wind Power, Oslo 2002, 7p

[7] Jenkins N, Allan R, Crossley P, Kirschen D, Strbac G.: Embedded generation, IEE Power and Energy series 31, London UK, 2000, 273p

[8] Erlich I, Wrede H, Feltes C.: Dynamic behavior of DFIG-based wind turbines during grid faults, IEEE Power Conversion Conference Nagoya 2007, pp. 1195-1200

[9] Erlich I, Wilch M, Feltes C.: Reactive power generation by DFIG based wind farms with AC grid connection, EPE 2007, pp. 1-10

[10] Gong B, Xu D, Wu, B.: Cost effective method for DFIG fault ride-through during symmetrical voltage dip, IECON 2010, pp. 3269-3274

[11] Kasem A.H, El-Saadany E.F, El-Tamaly H.H, Wahab M.A.A.: An improved fault ride through strategy for doubly fed induction generator-based wind turbines, IET Renewable Power Generation, Vol 2, no 4, 2008, pp. 201-214

[12] Xiang D, Ran L, Tavner P.J and Yang S.: Control of a doubly fed induction generator in a wind turbine during grid fault ride-through", IEEE Transactions on Energy Conversion, Vol 21 no. 3, 2006, pp. 652-662.

[13] Mäkinen A.S, Raipala O, Mäki K, Repo S, Tuusa H.: Fault ride-through capability of full-power converter wind turbine, Journal of Energy and Power Engineering, Vol. 4, no 10, 2010, 17 p.

[14] Teodorescu R, Liserre M, Rodriguez P.: Grid converters for photovoltaic and wind power systems, John Wiley & Sons, Ltd. 2011. 398p

[15] Mäkinen A.S, Tuusa H.: Effect of transient flux compensation control on fault ride through of doubly fed induction generator wind turbine, ICREPQ 2011, Las Palmas, Spain, 6p.